

# Nano Friction Behavior of Electroless Nickel Phosphorus Coatings

Mizan Ahmed<sup>a</sup>, Prasanta Sahoo<sup>a</sup>, Suman Kalyan Das<sup>a,\*</sup>

<sup>a</sup>Department of Mechanical Engineering, Jadavpur University, Kolkata 700032, India.

## Keywords:

EN coating  
Nano tribology  
COF  
Ni-P  
Ni-P-W  
Ni-P-Cu

## ABSTRACT

Nano-tribology is a field that has gained significant relevance in the last few years. Electroless nickel (EN) coatings have shown huge potential for tribology-based applications. The present research investigates the nanotribological behavior of different EN coatings, namely Ni-P, Ni-P-W, and Ni-P-Cu. The study involves testing coated pin specimens against a suitable counterface. A nano tribometer is used to test the specimens and measure the coefficient of friction (COF). The experiments are conducted by varying the sliding velocity while maintaining a constant load and vice versa. The surface topography of the coatings is examined using Scanning Electron Microscope (SEM) and Energy Dispersive X-Ray Analysis (EDAX). The findings reveal similarities in the nano frictional behavior of the coatings to their behavior in macro scale.

## \* Corresponding author:

Suman Kalyan Das   
E-mail: [skdas.me@gmail.com](mailto:skdas.me@gmail.com)

Received: 6 September 2023

Revised: 23 October 2023

Accepted: 3 January 2024



© 2024 Published by Faculty of Engineering

## 1. INTRODUCTION

The central area of interest in nanotribology research pertains to the examination of frictional phenomena occurring at the atomic level, particularly in relation to contacts involving single asperity. The fundamental goal is to develop innovative approaches for managing friction and wear at macroscopic levels, which are pertinent to conventional engineering applications [1,2]. The discipline of nanotribology encompasses the investigation of essential sliding characteristics and involves contacts that vary from a few to several hundred nanometers in dimension [3]. The

field of nanotribology has witnessed substantial progress in recent decades, primarily attributed to the emergence of Nano electromechanical systems /Micro electromechanical systems (NEMS/MEMS) and technological advances in the fabrication of 2D materials [4]. At the nanoscale, the effects of the force of inertia are considered to be insignificant, while the dominant forces comprise Van der Waals forces, electrostatic forces, capillary forces, etc. [5,6]. NEMS, MEMS, magnetic recording disc drives, and other applications exhibit nanotribological phenomena. Nanotribology is characterized by a low load, a small mass, elastic deformation, and little to no wear. Nano-

tribometers, friction force microscopes, surface force apparatuses, and atomic force microscopes are all excellent tools for conducting nanotribological research [7].

Electroless nickel (EN) coating uses chemical reactions to deposit nickel alloys on a surface without electricity. The utilization of EN coating has gained widespread acceptance in various engineering applications globally due to its numerous benefits. The primary areas of utilization for these coatings include the aerospace, automotive, electronics, oil and gas, and medical industries. The coating exhibits distinctive attributes such as exceptional resistance to corrosion, wear, and abrasion, as well as lubricative, ductile, and electrical properties [8,9]. Unlike electroplating, which requires more power and machinery to give a material (often steel) a durable and high-quality finish, electroless nickel coating requires neither. It's faster and more precise. The fact that no electrical energy is required makes it an economical choice. Industries often use Ni-P plating because of the coating's high density, good corrosion resistance, and durability [10,11]. The increase in phosphorus (P) content results in a rise in the microhardness of the coatings [12]. Moreover, the Ni-P coatings can be customized by introducing several secondary elements into the main matrix. Several coatings, viz. Ni-Mo-P, Ni-P-W, etc. have been successfully developed that have their own special set of characteristics and offer their own set of advantages. The comparative analysis demonstrates that the Ni-P-W coatings possess an enhanced degree of hardness and resistance to wear when compared to the Ni-P coatings. The incorporation of copper (Cu) into Ni-P alloys has been found to enhance their corrosion resistance, as reported in the literature [13,14]. Now, the coated surfaces often experience intense sliding contact, leading to tribological failure. The onset of this failure is commonly initiated at the nano level on the surface. Subsequently, these failures become evident on the macroscopic scale, ultimately leading to damage to the protective coatings. The surface hardness of a coating plays a crucial role in determining its tribological outcome, as it is closely associated with several mechanical parameters such as strength, ductility, and durability against wear [15]. The incorporation of nanoparticles or composite coatings has been shown to enhance the hardness of materials [16,17]. Also, it has been observed that the hardness of a coating increases

up to a specific threshold temperature, above which it begins to decrease [18].

The importance of material surfaces serving as a connecting interface between materials and their surrounding environment is a crucial concept, especially in the field of nanotribology. When it comes to tribological processes, the performance, durability, and efficiency of machinery and systems are all significantly affected by the surface attributes of the materials used in their construction. The friction and wear properties of components in contact are influenced by the interaction of their surfaces. The behavior of friction and wear is greatly influenced by factors like surface roughness, hardness, and lubrication [19]. Coatings, treatments, and surface texturing are methods of surface modification utilized to improve the qualities of materials' surfaces for specific tribological applications [20]. In addition, it is essential to shield surfaces from corrosion and environmental conditions to stop the deterioration of materials [21]. Understanding and managing the adhesion forces between surfaces is crucial for applications like adhesives and MEMS/NEMS [22]. Overall, materials' surfaces improve machinery efficiency, durability, and dependability, highlighting the importance of surface engineering and analysis in optimizing material interactions with their environment.

In the preceding discussion, the application of EN coatings in the field of macro tribology is discussed. In the contemporary era, significant advancements have been made in the field of nanotribology. The field of nanotribology plays a crucial role in the advancement of MEMS and NEMS across the semiconductor manufacturing industry, leading to enhanced device performance and reliability [23]. It also helps biomedical researchers investigate friction and wear in biological surfaces like articular cartilage, which improves prosthetic joints and helps understand disorders like osteoarthritis [24]. Nanotribology enables the aerospace sector to develop lightweight materials and sophisticated coatings to reduce friction and wear [25]. Nanotribology is needed to understand how hard drive read/write heads interact with magnetic disks and build high-density data storage technologies like phase-change memory [26]. Yet, research focused on evaluating the

nanotribological behavior of EN coatings is still at a relatively undeveloped stage. The objective of the present study is thus to examine the frictional properties of EN coatings at the nanoscale. The tiny, pin-shaped specimens are meticulously prepared and subsequently undergo the coating process. The pin sample is mounted to a pin-on-disc nanotribometer in order to conduct testing. The experimental procedure consisted of evaluating the frictional coefficient at various levels of loading and speeds. Following that, the tested samples undergo analysis utilizing Scanning Electron Microscopy (SEM) and Energy Dispersive X-ray Analysis (EDAX) methodologies to elucidate the characteristics of the surface morphology and composition, respectively.

## 2. EXPERIMENT DETAILS

### 2.1 Development of coating

Three different electroless nickel alloy coatings are prepared and characterized in this work. The coatings include electroless Ni-P, Ni-P-W and Ni-P-Cu. The substrate for the EN coatings is a solid cylindrical piece of mild steel with a diameter of 2 mm and a length of 10 mm. The present work mainly attempts to investigate the tribological behavior of electroless nickel coatings at nanoscale. The substrate material is chosen mainly for the development of the coating and to provide the necessary strength during testing and characterization. As mild steel is commonly available at a lower cost, the same is selected as the substrate material. The substrates were

polished to maintain a smooth surface finish of grade N5 ( $R_a = 0.40 \mu\text{m}$ ). Only substrates displaying negligible variations in roughness (specifically less than 0.1%) are selected for the deposition of the coating. Subsequently, each substrate is cleaned with soap and water, followed by the elimination of any remaining organic residue using acetone. To enhance the elimination of corrosion and surface oxide films before coating, the pin samples go through a short pickling process involving a one-minute immersion in a solution with 50% HCl. Following the cleaning steps, the substrates are activated in a solution containing palladium chloride ( $\text{PdCl}_2$ ) at a temperature of  $50^\circ\text{C}$ . Subsequently, they are immersed in the respective electroless baths for 1.5h. Considering the surface area of the substrate to be around  $69.11 \text{ mm}^2$ , the bath load translates to about  $7 \text{ cm}^2/\text{L}$ .

Fig. 1 shows a schematic configuration of the EN deposition setup, and Table 1 displays the bath components and deposition parameters for each coating. For achieving uniformity in coating thickness, variables including deposition time and bath volume are kept constant. Once the deposition process is completed, the specimens are cleaned with water. The hardness of the samples is determined using a Vickers tester (VMHT MOT, Technische Mikroskopie, Germany) at a low load of 100 g-f for a dwell time of 15 s at  $25 \mu\text{m/s}$  speed. The center line average roughness ( $R_a$ ) of the coatings is measured by using a stylus type (Surtronic 3+, Taylor Hobson, Leicester, UK) profilometer. With 0.8 mm sampling length, 4 mm traverse length, and 1 mm s<sup>-1</sup> traverse speed.

**Table 1.** Composition of the EN coating baths and their operating parameters.

Bath constituents and operating parameters	Ni-P	Ni-P-Cu	Ni-P-W	Function(s)
$\text{NiSO}_4 \cdot 6\text{H}_2\text{O}$	20 g/l	25 g/l	25 g/l	Source of Nickel
$\text{NiCl}_2 \cdot 6\text{H}_2\text{O}$	20 g/l	-	-	Source of Nickel
$\text{NaPO}_2\text{H}_2$	10-24 g/l	15 g/l	17 g/l	Source of Phosphorus and Reducing Agent
$\text{C}_4\text{H}_4\text{Na}_2\text{O}_4$	12 g/l	-	-	Reducing Agent
$\text{Na}_3\text{C}_6\text{H}_5\text{O}_7$	-	-	35 g/l	Complexing agent
$(\text{NH}_4)_2\text{SO}_4$	-	-	30 g/l	Buffering agent
$\text{Na}_2\text{WO}_4$	-	-	5-25 g/l	Source of Tungsten
$\text{CuSO}_4 \cdot 5\text{H}_2\text{O}$	-	15 g/l	-	Source of Copper
Temperature	$90^\circ\text{C}$	$90^\circ\text{C}$	$90^\circ\text{C}$	-
Coating duration	1.5h	1.5h	1.5h	-
Volume of bath	100 ml	100 ml	100 ml	-

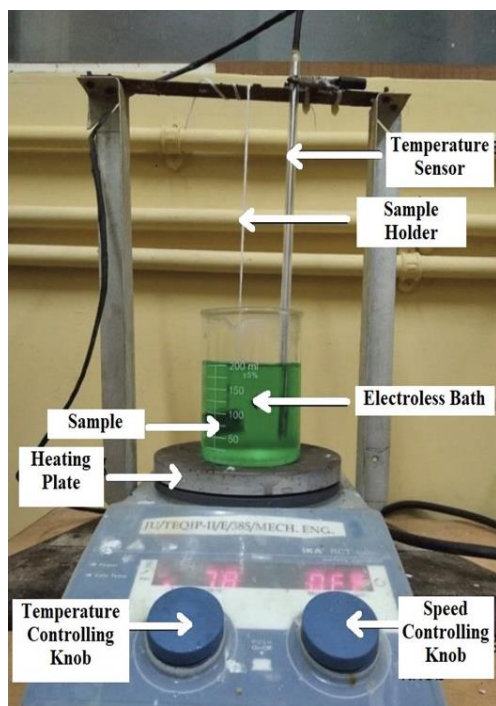


Fig. 1. Electroless nickel deposition setup.

Table 2. Process parameters and their values.

Parameter	Value
Normal force range	100 mN to 800 mN
Rotating speed	40 rpm to 100 rpm
Track radius	3 mm

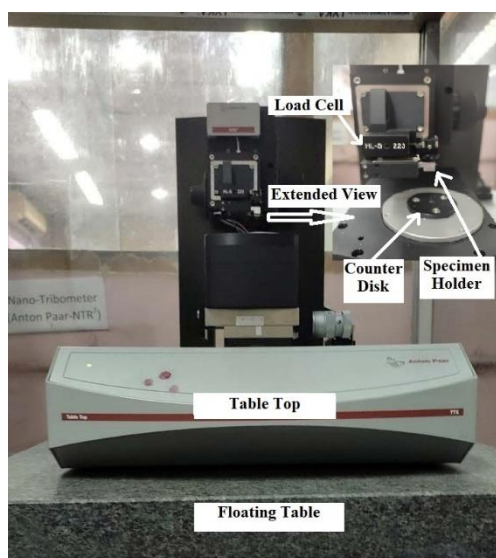


Fig. 2. A photograph of the nanotribometer.

## 2.2 Nanotribological tests of EN coatings

The nanotribological behavior of the coated samples is determined by testing them at room temperature (32°C) in a pin-on-disc type nanotribometer (Anton Paar NTR3, Austria)

under dry conditions. Fig. 2 shows an in-depth look at the instrument, complete with labels. The pin samples are positioned in a vertical orientation within the load cell of the nanotribometer, whereas a square counterface (10mm × 10mm) made of hardened steel is mounted on a revolving disc of the nanotribometer which slides against the EN-coated pins. It runs on a 3.0 mm-wide track radius. A load cell capable of measuring up to 1000 mN is used to calculate the frictional force. Table 2 presents the process parameters along with their corresponding values used for testing the coated samples. Tests were performed under varying loads, keeping the speed constant (at 70 rpm) as well as under varying speeds keeping the load constant (at 400mN). It is to be noted that in the present study, for every test, a new sample is used. There is no repetition of the used sample. However, for repeatability, at least three samples were used at each test condition.

## 2.3 Microstructural study of coatings

In this investigation, a field-emission scanning electron microscope (FESEM, Zeiss, Ultra 55, Germany) was employed to investigate the microstructure and surface morphology of the EN coatings. Energy-dispersive X-ray analysis is utilized with the purpose of identifying the composition of the coatings, particularly in relation to the proportional weights of nickel, phosphorus, and other expected constituent elements.

## 3. RESULTS AND DISCUSSION

### 3.1 Microhardness and surface roughness study

The microhardness and surface roughness of the uncoated and coated samples are provided in Table 3. It is found that the hardness of the samples increases significantly post deposition of the coatings. The highest hardness is displayed by Ni-P-W coatings considering the incorporation of harder W in the coating matrix. As far as the roughness is concerned, the coatings are found to display similar roughness value as the substrates. This complies with the fact that EN coatings are known to follow the substrate surface profile.

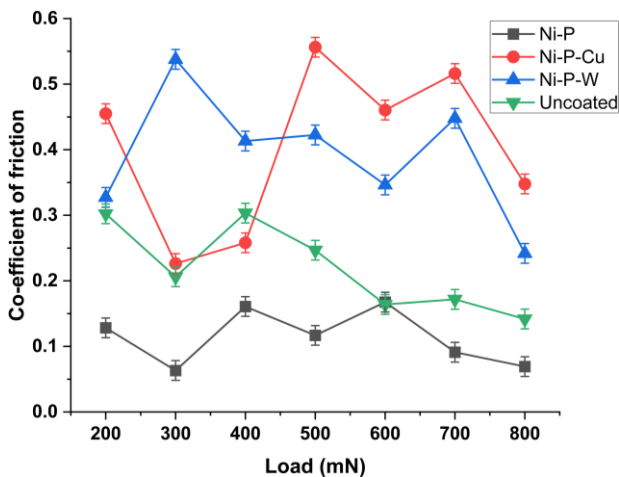
**Table 3.** Microhardness and surface roughness of samples.

Sample	Microhardness (HV <sub>0.1</sub> )	Surface Roughness, R <sub>a</sub> (μm)
Uncoated	168±8	0.40
Ni-P	582±12	0.46
Ni-P-Cu	522±11	0.43
Ni-P-W	670±14	0.42

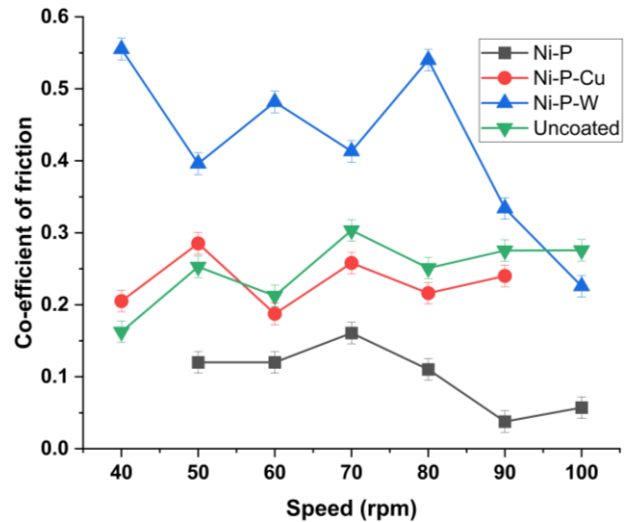
### 3.2 Nanofriction behavior study of the coatings

All three coatings, together with uncoated samples, were evaluated in the nanotribometer. The experiment involved recording the real-time coefficient of friction (COF) value for all the samples. Unfortunately, wear data could not be acquired due to the minimal weight reduction experienced by the specimens.

Fig. 3(a) and Fig. 3(b) illustrate the influence of applied load and sliding speed, respectively, on the nanofriction behavior of EN coatings and uncoated samples. For Ni-P coatings, both plots displayed an undulating pattern, although they demonstrated a gradual decrease in COF with a rise in applied load and sliding speed. For Ni-P-Cu coatings, no particular trend could be identified. However, Ni-P-W exhibit similar undulating patterns like Ni-P as an overall decreasing trend in the case of both the load and speed plots. Non-coated specimens also do not show a noticeable trend. However, COF shows a gradual decrease with a rise in the applied load while increasing with a rise in the sliding speed.



(a)



(b)

**Fig. 3.** COF vs. (a) applied load and (b) speed plots of coated and uncoated samples.

A contributing factor to the occurrence of undulation observed in COF plots may be the vaporization of absorbed water at the contacting region between the pin and counterface [7]. The pin and its counterface are disconnected when condensation of atmospheric water occurs.

The occurrence of this phenomenon leads to the development of a water bridge, or meniscus, between the two surfaces. During the testing process, the occurrence of sliding resulted in the generation of heat, which caused the water bridge at the intersection to go through a phase transition into a gaseous state. Subsequently, contact between the sample and the counterface is established. If a water bridge is created again, the contact will break. This results in the undulation in the COF plots.

An additional possible explanation could involve the generation of wear debris at the contact interface [27]. When subjected to high loads, the repetitive sliding of a pin against a hard counterpart leads to wear. The phenomenon of wear results in the production of minute wear particles. As the pin slides across the surface, wear debris becomes embedded and rolls between the pin and its counterpart. As a result of this phenomenon, friction decreases under elevated loads [27].

Another potential factor could be the generation of heat. The sliding of a pin over its counterpart results in the generation of heat at the junction



between the two surfaces. The heat generation processes have the potential to impact various material properties, including stress response and

adhesion. The alteration in characteristics yielded a decrease in friction under high load conditions, as reported in previous literature [28].

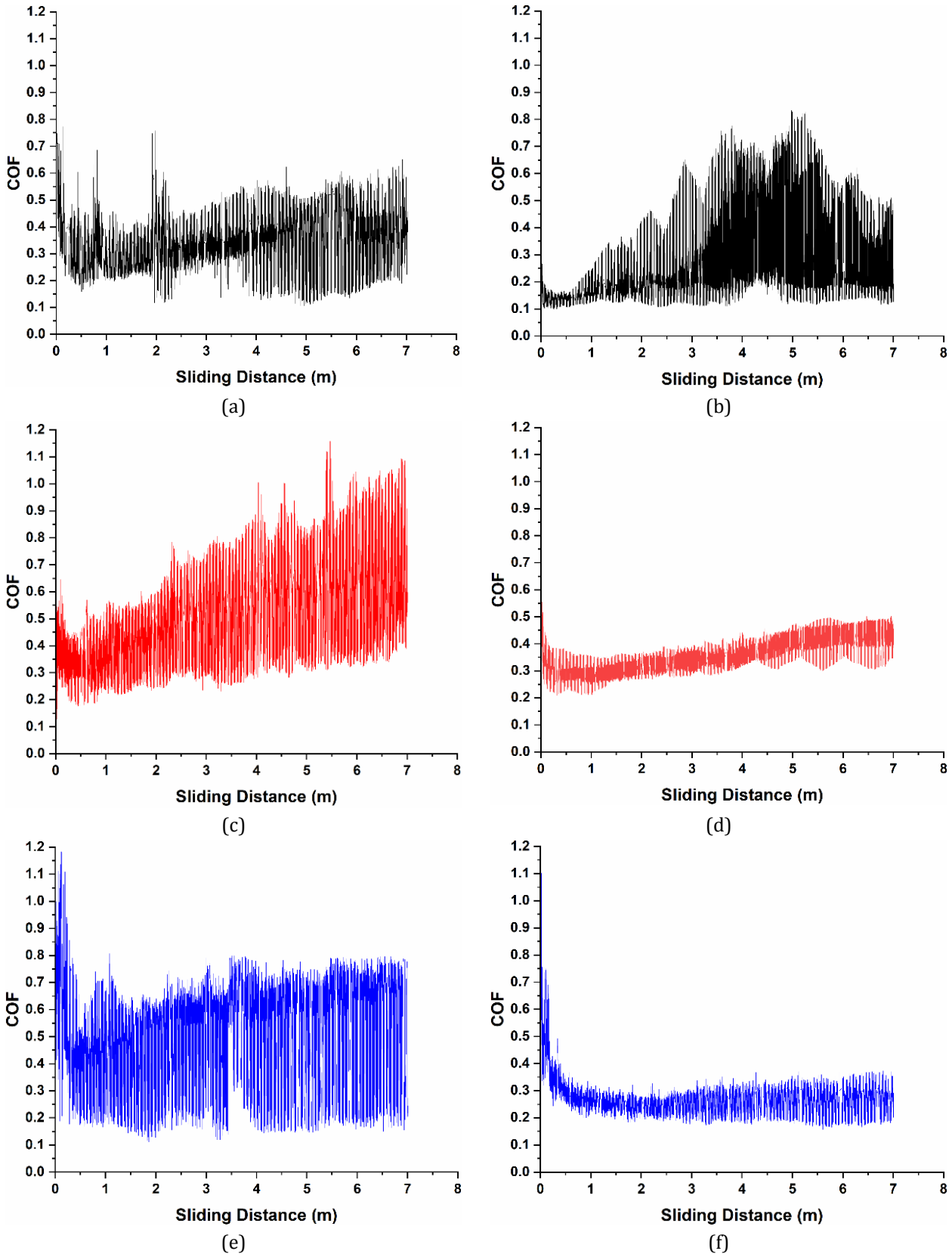


**Fig. 4.** COF vs sliding distance plots of (a) Ni-P(Max), (b) Ni-P(Min) (c) Ni-P-Cu (Max), (d) Ni-P-Cu (Min), (e) Ni-P-W(Max), (f) Ni-P-W(Min) samples.

At the nanoscale, the frictional force is reliant upon the adhesion force existing between the surfaces, besides the normal force. The connection between the normal force and the COF resulting from adhesion does not exhibit a linear relationship. In the context of low loads, adhesion emerges as the dominant mechanism, whereas for higher loads, the ploughing effect and deformation assume the primary functions in governing the system [7]. Moreover, as already mentioned several types of surface forces, encompassing Van der Waals forces, magnetic, capillary, forces, etc. arise upon proximity to the counterbody. When viewed on a nanoscale, their magnitude is significant. These types of surface forces have the potential to significantly affect the friction behavior of the samples [7].

Fig. 4 shows the variation of COF over sliding distance for all the coatings. All of the plots exhibit an initial high COF that subsequently stabilizes at a somewhat stable COF value, with the exception of the Ni-P-Cu (Max) and Ni-P (Min) cases. They exhibit a slight rise in COF rather a stable value. The phrases "Max" and "Min", respectively, represent the results of the samples displaying the highest and lowest COF for each coating.

Overall, from the friction results, it can be observed that the EN coating increases the COF of the mild steel sample to some extent. The results clearly indicate that Ni-P coatings exhibit a comparatively lower frictional coefficient. The findings suggest that Ni-P-W displays a higher COF for specific initial loads, whereas Ni-P-Cu exhibits a greater COF for larger loads. Nevertheless, the uncoated samples demonstrate a more or less COF within the load range. A similar trend is observed in the COF vs speed case. From the results, it can be said that the incorporation of ternary elements in Ni-P coating affects its nanotribological behavior.

### 3.3 Microstructural study of the worn surfaces

The FESEM micrographs of the tested coatings are presented in Fig. 5. The phrases "Max" and

"Min" represent the samples, as explained before. Both the samples exhibiting the maximum and minimum COFs are assessed for understanding the underlying tribological mechanisms and spot differences, if any. In Ni-P coatings, the usual nodular morphology seems to be flattened on the test track. In fact, a closer look at the micrograph reveals fine wear tracks representative of abrasive ploughing. Besides, pits and prows are observed which imply the adhesive wear mechanism is also in action. In the case of Ni-P-Cu, a blistered morphology is noticed (refer to Fig. 5c). However, remnants of nodular morphology are also observed (refer to Fig. 5d). In fact, some minor cracks are also observed in the sliding zone. For the Ni-P-W coating, the surface seems very smooth with over. Wear debris is noticed, particularly for the sample displaying a minimum COF, which indicates the occurrence of 3-body abrasion. The nodular surface of EN coatings in general is related to lower COF display [29]. Coatings with a nodular surface topography exhibit a reduced contact area in comparison to their flat surfaces. The reduction of friction occurs due to the decrease in the area of contact [30,31]. This may partly explain the lower COF displayed by the Ni-P-W sample shown in Fig. 5f. Similar findings have been previously reported by others [27]. Table 4 presents the compositions of the tested coatings as observed through EDAX analysis. From the results, it can be seen that all the coatings are in the high phosphorus category and hence expected to have an amorphous microstructure [8]. The detection of iron is an interesting finding, as considering the deposition thickness (around 30 $\mu$ m), the iron from the ferrous substrate is not expected to be detected. Hence, the iron has come from the steel counterface due to the high mutual solubility between nickel and iron. This phenomenon is aggravated in the presence of adhesive wear mechanism. It may be further observed that iron detection is relatively higher in samples that exhibit higher COF values. This may imply that a higher COF is experienced when the adhesive wear mechanism is active.

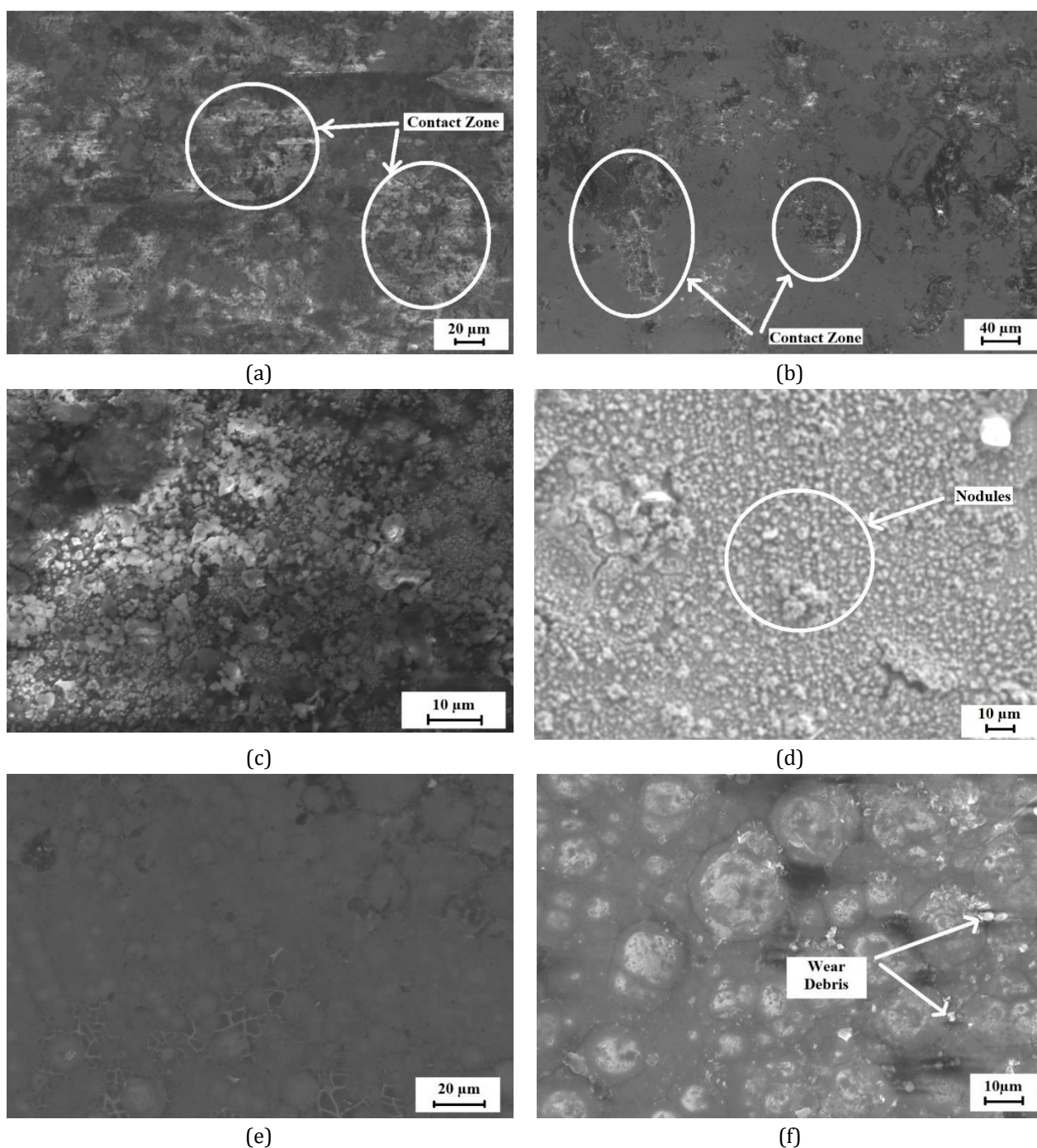


**Fig. 5.** SEM micrograph of Ni-P, Ni-P-Cu and Ni-P-W coatings. (a) Ni-P(Max), (b) Ni-P(Min) (c) Ni-P-Cu (Max), (d) Ni-P-Cu (Min), (e) Ni-P-W(Max), (f) Ni-P-W(Min).

**Table 4.** Weight percentage of different elements found in EDAX.

Elements	Ni-P (Max) (wt%)	Ni-P (Min) (wt%)	Ni-P-Cu (Max) (wt%)	Ni-P-Cu (Min) (wt%)	Ni-P-W (Max) (wt%)	Ni-P-W (Min) (wt%)
Ni	87.11	88.14	78.25	79.16	80.02	81.12
P	9.76	10.30	10.18	11.09	9.52	10.59
Cu	-	-	7.73	8.02	-	-
W	-	-	-	-	8.31	8.17
Fe	3.13	1.56	3.84	1.73	2.15	0.12



### 3.4 Comparison with macroscopic friction behavior of the coatings

Nanotribology research is a relatively new advancement compared to the well-established discipline of macro tribology. In order to conduct a comparative analysis, the friction behavior of the three EN coatings was examined under varying load and speed conditions at a macroscopic level. Fig. 6 illustrates the friction behavior of the coatings across a range of load and speed conditions observed at the macro scale [32]. In all cases involving macro and nano testing, it is clear that the inclusion of ternary elements, viz. tungsten or copper, raises the COF of Ni-P coatings. In the case of macro testing, Ni-P-W exhibits the highest COF. Ni-P-Cu on the other hand displays a COF of intermediate magnitude.

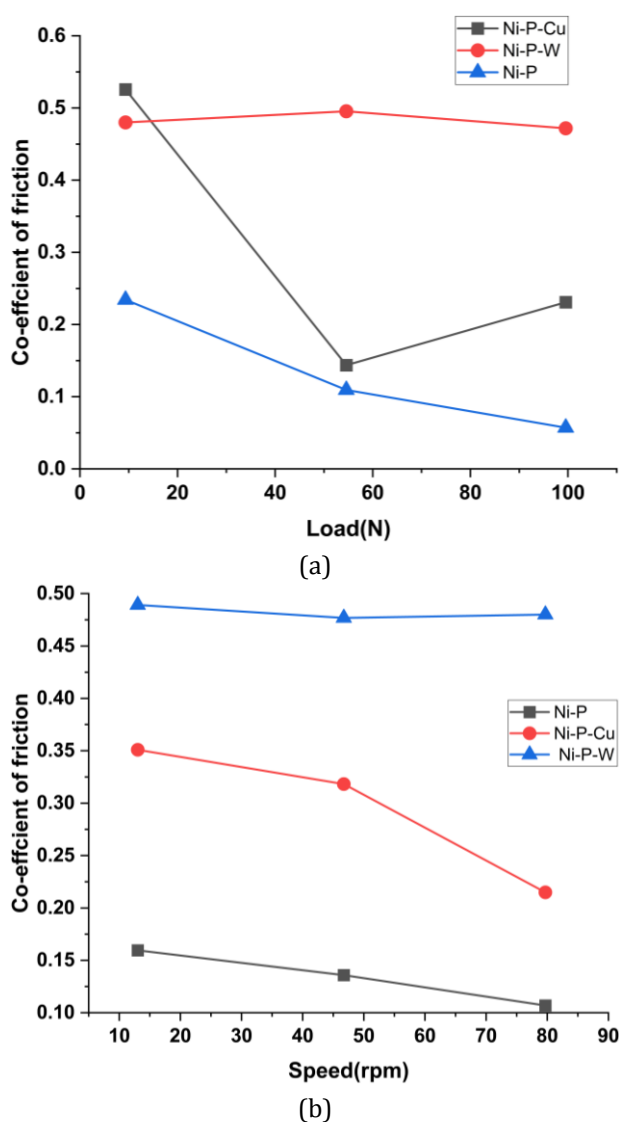


Fig. 6. Variation of (a) COF with load and (b) COF vs speed at macro tests (adapted from [31])

When subjected to various speeds and loads (as shown in Figure 6), the coefficient of friction (COF) for Ni-P-Cu and Ni-P-W consistently

follows an intermediate and highest trend, respectively, in both macro and nano tests. The COF for the Ni-P coating consistently remains lower than that of the ternary coatings across all instances, encompassing both macro and nano scales. In a nutshell, it can be seen that the COF exhibits a comparable pattern for both macro and nano tests for all coatings.

### 4. CONCLUSIONS

The present article investigates the nano friction behavior exhibited by various EN coatings (Ni-P, Ni-P-Cu, and Ni-P-W) under different load and speed conditions. The following conclusions can be drawn from the work:

- The coatings raise the COF of the mild steel substrates.
- The friction plots obtained for the coatings do not exhibit a clear trend over the speed and load range used in the present investigation.
- Incorporation of W and Cu as ternary elements tends to enhance the friction of EN coatings. Ni-P-W exhibits the highest COF, Ni-P-Cu follows an intermediate trend, and Ni-P displays the lowest one.
- The nano friction behavior of the coatings has a good similarity with the friction behavior observed in the micro tests. Overall, Ni-P-W exhibits the highest COF among the coatings.

It is worth noting that nanotribology is a relatively new field of study, and while EN coatings have shown promising tribological performance on a larger scale, their applicability on the micro and nanoscales requires further investigation. Further study is required in the future in order to enhance our comprehension of the friction behavior exhibited by these coatings when examined at nano scales.

### ORCID iDs

Mizan Ahmed  0009-0001-6883-1228  
 Prasanta Sahoo  0000-0002-1538-0646  
 Suman Kalyan Das  0000-0001-7540-7954

## REFERENCES

- [1] B. Bhushan, J. N. Israelachvili, and U. Landman, "Nanotribology: friction, wear and lubrication at the atomic scale," *Nature*, vol. 374, no. 6523, pp. 607–616, Apr. 1995, doi: [10.1038/374607a0](https://doi.org/10.1038/374607a0).
- [2] I. Szlufarska, M. Chandross, and R. W. Carpick, "Recent advances in single-asperity nanotribology," *Journal of Physics D: Applied Physics*, vol. 41, no. 12, p. 123001, May 2008, doi: [10.1088/0022-3727/41/12/123001](https://doi.org/10.1088/0022-3727/41/12/123001).
- [3] B. Bhushan, "Nanotribology and nanomechanics," *Wear*, vol. 259, no. 7–12, pp. 1507–1531, Jul. 2005, doi: [10.1016/j.wear.2005.01.010](https://doi.org/10.1016/j.wear.2005.01.010).
- [4] A. Vanossi et al., "Recent highlights in nanoscale and mesoscale friction," *Beilstein Journal of Nanotechnology*, vol. 9, pp. 1995–2014, Jul. 2018, doi: [10.3762/bjnano.9.190](https://doi.org/10.3762/bjnano.9.190).
- [5] S. H. Kim, D. B. Asay, and M. T. Dugger, "Nanotribology and MEMS," *Nano Today*, vol. 2, no. 5, pp. 22–29, Oct. 2007, doi: [10.1016/s1748-0132\(07\)70140-8](https://doi.org/10.1016/s1748-0132(07)70140-8).
- [6] R. Maboudian and R. T. Howe, "Critical Review: Adhesion in surface micromechanical structures," *Journal of Vacuum Science & Technology B*, vol. 15, no. 1, pp. 1–20, Jan. 1997, doi: [10.1116/1.589247](https://doi.org/10.1116/1.589247).
- [7] S.K. Sinha, N. Satyanarayana, S. C. Lim, *Nanotribology and Materials in MEMS*, Heidelberg: Springer, 2013.
- [8] P. Sahoo, S.K. Das, "Tribology of electroless nickel coatings—a review," *Materials & Design*, vol. 32, no. 4, pp. 1760–1775, 2011, doi: [10.1016/j.matdes.2010.11.013](https://doi.org/10.1016/j.matdes.2010.11.013).
- [9] Z. Karaguiozova, J. A. Kaleicheva, V. Mishev, and G. Nikolcheva, "Enhancement in the tribological and mechanical properties of electroless Nickel Nanodiamond coatings plated on iron," *Tribology in Industry*, vol. 39, no. 4, pp. 444–451, Dec. 2017, doi: [10.24874/ti.2017.39.04.03](https://doi.org/10.24874/ti.2017.39.04.03).
- [10] S. K. Das, P. Sahoo, "Electroless Nickel Phosphorus Deposits," in *Electroless Nickel Plating: Fundamentals to Applications*, F. Delaunois, V. Vitry, L. Bonin, Eds. Boca Raton: CRC Press, pp. 89–171, 2019.
- [11] S. Roy, P. Sahoo, "Tribological Performance Optimization of Electroless Ni-P-W Coating Using Weighted Principal Component Analysis," *Tribology in Industry*, vol. 35, no. 4, pp. 297–307, 2013.
- [12] M. S. Safavi, M. Fathi, and I. Ahadzadeh, "Feasible strategies for promoting the mechano-corrosion performance of Ni-Co based coatings: Which one is better?," *Surface and Coatings Technology*, vol. 420, p. 127337, Aug. 2021, doi: [10.1016/j.surfcoat.2021.127337](https://doi.org/10.1016/j.surfcoat.2021.127337).
- [13] Q. Zhao, Y. Liu, and E. W. Abel, "Effect of Cu content in electroless Ni-Cu-P-PTFE composite coatings on their anti-corrosion properties," *Materials Chemistry and Physics*, vol. 87, no. 2–3, pp. 332–335, Oct. 2004, doi: [10.1016/j.matchemphys.2004.05.028](https://doi.org/10.1016/j.matchemphys.2004.05.028).
- [14] Q. Zhao, Y. Liu, and E. W. Abel, "Surface free energies of electroless Ni-P based composite coatings," *Applied Surface Science*, vol. 240, no. 1–4, pp. 441–451, Feb. 2005, doi: [10.1016/j.apsusc.2004.07.013](https://doi.org/10.1016/j.apsusc.2004.07.013).
- [15] A. Kumar, S. K. Nayak, A. Pathak, A. Banerjee, and T. Laha, "Investigation of nanomechanical deformation behavior in plasma sprayed Fe based amorphous/ nanocrystalline composite coating via multi-scale indentation and nanotribology," *Journal of Non-Crystalline Solids*, vol. 545, p. 120244, Oct. 2020, doi: [10.1016/j.jnoncrysol.2020.120244](https://doi.org/10.1016/j.jnoncrysol.2020.120244).
- [16] M. S. Safavi, A. Rasooli, and F. A. Sorkhabi, "Electrodeposition of Ni-P/Ni-Co-Al<sub>2</sub>O<sub>3</sub> duplex nanocomposite coatings: towards improved mechanical and corrosion properties," *Transactions of the IMF*, vol. 98, no. 6, pp. 320–327, Sep. 2020, doi: [10.1080/00202967.2020.1802106](https://doi.org/10.1080/00202967.2020.1802106).
- [17] A. Araghi and M. H. Paydar, "Electroless deposition of Ni-P-B<sub>4</sub>C composite coating on AZ91D magnesium alloy and investigation on its wear and corrosion resistance," *Materials & Design*, vol. 31, no. 6, pp. 3095–3099, Jun. 2010, doi: [10.1016/j.matdes.2009.12.042](https://doi.org/10.1016/j.matdes.2009.12.042).
- [18] Y. Wu, H. Liu, B. Shen, L. Liu, and W. Hu, "The friction and wear of electroless Ni-P matrix with PTFE and/or SiC particles composite," *Tribology International*, vol. 39, no. 6, pp. 553–559, Jun. 2006, doi: [10.1016/j.triboint.2005.04.032](https://doi.org/10.1016/j.triboint.2005.04.032).
- [19] F. P. Bowden and D. Tabor, *The Friction and Lubrication of Solids*, Oxford: Oxford University Press, 2001.
- [20] B. Bhushan, *Introduction to Tribology*, 2<sup>nd</sup>ed. New York: John Wiley & Sons, 2013.
- [21] P. R. Roberge, *Handbook of Corrosion Engineering*, 3<sup>rd</sup>ed. New York: McGraw-Hill Education, 2019.
- [22] J. N. Israelachvili, *Intermolecular and Surface Forces*, 3<sup>rd</sup>ed. San Diego: Academic Press, 2011.
- [23] B. Bhushan, *Nanotribology and nanomechanics: An Introduction*, 3<sup>rd</sup>ed. Heidelberg: Springer, 2011.
- [24] S. Wang, K. Liu, X. Yao, and L. Jiang, "Bioinspired Surfaces with Super wettability: New Insight on Theory, Design, and Applications," *Chemical Reviews*, vol. 115, no. 16, pp. 8230–8293, Aug. 2015, doi: [10.1021/cr400083y](https://doi.org/10.1021/cr400083y).

- [25] J. M. Martin and A. Erdemir, "Superlubricity: Friction's vanishing act," *Physics Today*, vol. 71, no. 4, pp. 40–46, Apr. 2018, doi: [10.1063/pt.3.3897](https://doi.org/10.1063/pt.3.3897).
- [26] B. Bhushan, "Nanotribology and nanomechanics of MEMS/NEMS and BioMEMS/BioNEMS materials and devices," *Microelectronic Engineering*, vol. 84, no. 3, pp. 387–412, Mar. 2007, doi: [10.1016/j.mee.2006.10.059](https://doi.org/10.1016/j.mee.2006.10.059).
- [27] M.A. Chowdhury, M.K. Khalil, D.M. Nuruzzaman, M. L. Rahaman, "The effect of sliding speed and normal load on friction and wear property of aluminum," *International Journal of Mechanical & Mechatronics Engineering*, vol. 11, no. 01, pp. 45–49, 2011.
- [28] D. M. Nuruzzaman and M. A. Chowdhury, "Effect of load and sliding velocity on friction coefficient of aluminum sliding against different Pin materials," *American Journal of Materials Science*, vol. 2, no. 1, pp. 26–31, Feb. 2012, doi: [10.5923/j.materials.20120201.05](https://doi.org/10.5923/j.materials.20120201.05).
- [29] A. Mukhopadhyay, T. K. Barman, and P. Sahoo, "Friction and Wear Performance of Electroless Ni-B Coatings at Different Operating Temperatures," *Silicon*, vol. 11, no. 2, pp. 721–731, Mar. 2018, doi: [10.1007/s12633-017-9678-y](https://doi.org/10.1007/s12633-017-9678-y).
- [30] D. K. Cohen PhD, "If you need less sliding friction, should you make the surface rougher or smoother?," *2017-01-03 | Quality Magazine*, Jan. 03, 2017. [Online]. Available: <https://www.qualitymag.com/articles/93749-if-you-need-less-sliding-friction-should-you-make-the-surface-rougher-or-smoother>
- [31] Maksim Prozhega, Egor Reschikov, Egor Konstantinov, "The Technological Factors and Operating Conditions Influence on the Molybdenum Disulfide Coatings Tribological Properties," *Journal of Materials and Engineering*, vol. 1, iss. 4, pp. 159-163, 2023, doi: [10.61552/JME.2023.04.003](https://doi.org/10.61552/JME.2023.04.003).
- [32] P. Sahoo and S. Roy, "Tribological behavior of electroless Ni-P, Ni-P-W and Ni-P-CU coatings," *International Journal of Surface Engineering and Interdisciplinary Materials Science*, vol. 5, no. 1, pp. 1–15, Jan. 2017, doi: [10.4018/ijseims.2017010101](https://doi.org/10.4018/ijseims.2017010101).